Front. Earth Sci. 2024, 18(4): 763−781
https://doi.org/10.1007/s11707-024-1116-z

RESEARCH ARTICLE

Applying 3D geological modeling to predict favorable areas for coalbed methane accumulation: a case study in the Qinshui Basin

Xiongxiong YANG[1,2,3], Shuheng TANG (✉)[1,2,3], Songhang ZHANG[1,2,3], Zhaodong XI[1,2,3], Kaifeng WANG[1,2,3], Zhizhen WANG[1,2,3], Jianwei LV[1,4]

1 School of Energy Resource, China University of Geosciences (Beijing), Beijing 100083, China
2 Key Laboratory of Marine Reservoir Evolution and Hydrocarbon Enrichment Mechanism (Ministry of Education), China University of Geosciences (Beijing), Beijing 100083, China
3 Key Laboratory of Strategy Evaluation for Shale Gas (Ministry of Land and Resources), China University of Geosciences (Beijing), Beijing 100083, China
4 Chinese Academy of Natural Resources Economics, Beijing 101149, China

Abstract Qinshui Basin possesses enormous deep coalbed methane (CBM) resources. Fine and quantitative description of coal reservoirs is critical for achieving efficient exploration and development of deep CBM. This study proposes a 3D geological modeling workflow that integrates three parts: geological data analysis, 3D geological modeling, and application of the model, which can accurately predict the favorable areas of CBM. Taking the Yushe-Wuxiang Block within the Qinshui Basin as a case study, lithology identification, sequence stratigraphy division, structural interpretation is conducted by integrating well logging, seismic, and drilling data. Six lithology types and regional structural characteristics of the Carboniferous-Permian coal-bearing strata are finely identified. Combining experimental testing on porosity and gas content and well testing on permeability, a 3D geological model that integrates the structural model, facies model, and property model was established. Utilizing this model, the total CBM resource volume in the study area was calculated to be 2481.3 × 10^8 m^3. Furthermore, the model is applied to predict the distribution ranges of four types of CBM favorable areas. The workflow is helpful to optimize well deployment and improve CBM resource evaluation, ultimately provide theoretical guidance for subsequent efficient exploration and development. Our study constitutes a reference case for assessing potential of CBM in other blocks due to the successful integration of multiple available of data and its practical applications.

Received August 19, 2023; accepted January 5, 2024

E-mail: tangsh@cugb.edu.cn

Keywords 3D geological modeling, CBM, fine reservoir characterization, Qinshui Basin, Yushe-Wuxiang Block

1 Introduction

Coalbed methane (CBM) is a significant natural gas resource that is widely distributed worldwide, with notable reserves in countries such as the United States, Australia, and China (Flores, 2014; Tao et al., 2019; Salmachi et al., 2021). The exploration and exploitation of CBM is of great significance for economic development and the improvement of energy structure (Moore, 2012; Qin et al., 2018). Currently, commercial CBM exploitation primarily focuses on shallow coal reservoirs with depths of around 1000 m. In recent years, significant progress has been made in the exploration and development of deep CBM reserves in blocks such as Linxing, Daning-Jixian and other blocks in the Ordos Basin, leading to the expansion of CBM exploration and development into deeper regions (Lu et al., 2021; Li and Li, 2022; Kang et al., 2023; Li et al., 2023a). China, possesses CBM resources, approximately 36.8 × 10^{12} m^3 buried at depths shallower than 2000 m. CBM with burial between 1000 and 2000 m accounts for 61.22% of the total resources, the development prospect of deep CBM is broad (Li et al., 2018b). In contrast to shallow, deep CBM is benefits from favorable geological conditions such as higher gas content, but low permeability. It is crucial to accurately predict favorable areas for CBM. However, due to the strong heterogeneity of coal reservoirs, a prerequisite for predicting favorable areas is a detailed description of the reservoir. Therefore, how can we

accurately characterize the property of coal reservoirs and predict favorable areas has become an urgent problem in the exploration and development of CBM.

Presently, various conventional methodologies have been employed for the comprehensive delineation of coal reservoirs, encompassing techniques such as logging assessments and seismic inversion. According to logging assessments, the gas content and its vertical variation can be acquired effectively at well locations, but it is difficult to obtain the lateral distribution characteristics especially in areas of lower exploration degree (Liu and Zhao, 2016). While certain geophysicists have ventured into predicting inter-well parameters through an analysis of seismic wave responses prompted by disparities in coal reservoir property, the precision of such prognostications remains constrained by seismic resolution (Liu et al., 2022a; Wei et al., 2023). In synopsis, the conventional reservoir characterization methods are generally encumbered by the scarcity of deep coal reservoir research data, encompassing well log data and core samples, potentially falling short of the envisaged predictive precision. Consequently, there is a pressing demand for the development of an approach that comprehensively integrates available data to accurately depict the spatial distribution of coal reservoir and their property.

3D geological modeling methods serve as effective tools for achieving precise and quantitative characterization of oil and gas reservoirs. Their primary advantage lies in their capability to simulation the intricate spatial distribution characteristics of heterogeneity reservoirs, thereby establishing a solid foundation for subsequent resource evaluation, numerical simulation, and development plan deployment. The method has been widely used in conventional oil and gas fields (Hu and Chugunova, 2008; Guo et al., 2015; Ali et al., 2022; Liu et al., 2022c). In recent years, scholars have directed their focus toward the significance of 3D geological modeling in characterizing CBM reservoirs. By utilizing the 3D geological model, the distribution characteristics of coal reservoir parameters such as thickness, gas content and coal body structure can be determined (Zhou et al., 2012; Zhou et al., 2020; Shu et al., 2023). Some scholars have also examined the influence of different geological modeling methods on CBM resource estimation and analyzed associated uncertainties (Karacan et al., 2012; Zhou et al., 2015; Duan et al., 2020). Several scholars have explored modeling workflows in the field. The four-step CBM modeling workflow incorporates multilevel constraints, but is specifically tailored for permeability modeling (Ma et al., 2018). Techniques grounded in quantitative analysis of logging and stratigraphy correlation enable fine-scale modeling of a single coal reservoir but ignore the merits and applicability of various simulation methods (Lv et al., 2020). Moreover, high-resolution geostatistical modeling is suitable for data-rich reservoirs. However, this approach is constrained by the lack of information in areas with a low density of well networks and is not well-suited for moderate to low exploration regions (Ren et al., 2019). Although 3D geological modeling can be done in CBM reservoirs easily using existing methods, the modeling accuracy under low density of well networks regions with moderate to low exploration levels still presents a big challenge. This issue significantly impacts the effective development of deep CBM and warrants further in-depth research.

In this study, the Yushe-Wuxiang Block is taken as an illustrative case, and a comprehensive workflow for 3D geological modeling is proposed. This workflow entails the integrated analysis of multi-source geological data from seismic, logging and drilling as geological constraints, and applied both deterministic and stochastic modeling methods to carry out 3D geological modeling of coal reservoirs. The model is also used to realize CBM resource estimation and favorable area prediction. The workflow can minimize the uncertainty due to the strong non-homogeneity of deep coal reservoirs and low density of well networks. It facilitates precise characterization of coal reservoirs, thereby significantly enhancing the accuracy of CBM favorable area predictions. Importantly, this workflow can be extended for application in other deep CBM blocks.

2 Methods

The technology for evaluating favorable areas of CBM

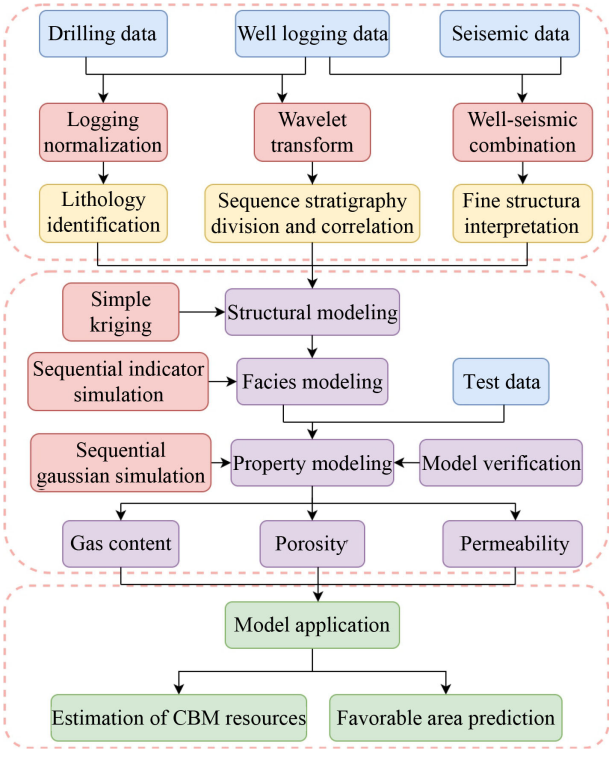

Fig. 1 Workflow for applying 3D geological modeling to predict favorable areas of CBM.

based on 3D geological modeling consists of three main components: geological data analysis, 3D geological modeling, and the application of the model (Fig. 1). Initially, it involves the integration of drilling, logging, and seismic data for geological data analysis. This process includes lithology identification based on logging normalization, sequence stratigraphy division and correlation based on wavelet transform, and fine structural interpretation using well-seismic combinations. These activities serve as the foundational data for 3D geological modeling. The 3D geological modeling technique comprises three pivotal approaches: structural modeling, achieved through indicator kriging; coal body structure modeling, realized via sequential indicator simulation; and property modeling, accomplished through sequential Gaussian simulation. Consequently, a 3D geological model is established, accurately reflecting real geological conditions. In the final stage, this 3D geological model is applied to estimate CBM resources and predict favorable areas.

2.1 Logging normalization

Due to the extensive study area and prolonged duration of logging, some CBM blocks have abnormal logging responses caused by logging instruments and environmental factors. Logging normalization can effectively eliminate errors, thereby improving the accuracy of lithology identification and minimize uncertainty in 3D geological modeling. Commonly employed logging normalization methods include the mean method, histogram method, trend surface method, and others. These methods are based on the principle that "formations of the same lithology at the same time exhibit similar logging responses". Through logging normalization, logging data from the same lithology strata within each well attain consistent mean values, frequency distribution, or exhibit regular patterns of change (Quartero et al., 2014; Rotimi et al., 2014; Li et al., 2020). Some scholars apply additional techniques such as frequency spectral decomposition and Hilbert transformation to further refine the accuracy of logging normalization (Ren et al., 2016).

Considering the study area's characteristics of significant well distances and consistent logging responses within the same lithology, the histogram method is chosen for logging normalization. Logging normalization is then conducted using a double standard layer, employing the following equation (Ren et al., 2016):

$$N_{\text{norm}} = R_{\min} + (R_{\max} - R_{\min})(N_{\log} - W_{\min})/(W_{\max} - W_{\min}), \quad (1)$$

where N_{norm} is the value of logging after normalization; $N_{\log}$ is the value of logging before normalization; $W_{\max}$ and $W_{\min}$ denote the logging values of the standard layer in each well, while $R_{\max}$ and $R_{\min}$ correspond to the logging values of the standard layer in the standard well.

2.2 Wavelet transform

Wavelet transform (WT) is a signal processing tool that can reveal hidden information in signals through the interpretation of time-frequency signals, can be used for geological interpretation. This study uses continuous wavelet transform (CWT), which is the main method of wavelet transform in analyzing well logging (Kadkhodaie and Rezaee, 2017). It is a convolution of the signal $f(t)$ with a set of functions generated by the mother wavelet $\psi(t)$. The CWT is calculated as follows (Zhu et al., 2023):

$$C(a,b,\psi(t),f(t)) = \frac{1}{\sqrt{|a|}}\int_{-\infty}^{+\infty} f(t)\psi\left(\frac{t-b}{a}\right)\mathrm{d}t, a \neq 0, \quad (2)$$

where C is the wavelet coefficient, a is scale parameter, b is position parameter, $\psi(t)$ is a wavelet function, and the $f(t)$ is the original signal, such as logging data.

Logging data contains important geological information, representing the superposition of multiple transgressive and regressive sedimentary cycles. Gamma ray (GR) logging is the primary target for CWT. By applying the CWT for multi-scale time-frequency analysis of GR logging, the wavelet coefficient curves and wavelet transformation reveal essential features that reflect the periodic changes in vertical sedimentary environment, sediment grain size, and hydrodynamic conditions. Therefore, analyzing the periodic variations in the wavelet coefficient curves and wavelet transformation provides insights into the response characteristics of interfaces and their corresponding relationship with sequence cycles. This approach enables the identification of key sequence boundaries and facilitates quantitative division of sequence stratigraphy (Kadkhodaie and Rezaee, 2017; Liang et al., 2019; Li et al., 2023b). For this study, the Morlet wavelet function, known for its strong periodicity and notable variability, is employed within the CWT.

2.3 Well-seismic combination

Structure features like faults and collapse columns significantly influence the continuity of coal reservoirs and the accumulation of CBM. Prior to conducting 3D geological modeling of the coal reservoir, a meticulous interpretation of the fine structures is crucial. When wells are sparsely distributed, the well-seismic combination method can make full use of the high lateral resolution of seismic data and the vertical resolution of well data, significantly improving the accuracy of structural interpretation. In this study, the Seismic Interpretation module within Petrel was utilized, employing logging data and seismic lines from the study area. Using the Seismic Interpretation module within Petrel, acoustic (AC) and density (DEN) logging were selected to generate synthetic seismic records. Horizon calibration was

performed by identifying prominent waveform features and strong energy associated with coal reservoir reflection waves. Faults were identified based on the signs of waveform displacement, discontinuity, and distortion. The identification of collapse columns relied on the observation of wave interruptions and disappearances within a limited range, enabling a detailed explanation of the structural characteristics.

2.4 Geological modeling methods

2.4.1 Simple Kriging

Kriging is an optimization interpolation method that uses linear least squares. It obtains data values for unsampled points by combining known data, with the data values being the weighted sum of adjacent data points, but without assuming any statistical distribution. The interpolation accuracy of Kriging depends on the number of known data points, and is suitable for deterministic modeling of relatively high-density data. The equation is (Zhou et al., 2015)

$$Z^*(u) = m + \sum_{\alpha=1}^{n(u)} \lambda_\alpha(u)[Z(u_\alpha) - m], \quad (3)$$

where $Z^*(u)$ represents the estimated value for estimation point u; $Z(u_\alpha)$ are the values of linear points; λ_α represents the value of the linear points weight; m denotes the mean from all the known points; $n(u)$ is the number of linear data points.

2.4.2 Sequential indicator simulation

Sequential indicator simulation (SIS) is a pixel-based stochastic simulation method that can be used for both discrete and continuous variables. The foundations of SIS are indicator transformation, indicator kriging, and sequential simulation. During the simulation process, the conditional probability distribution function is calculated for each grid in the 3D space. One of the key advantages of SIS is that it can encode soft data (well logging interpretation, geological reasoning and interpretation) for simulation, making it suitable for simulating geological phenomena with strong heterogeneity (Yong et al., 2020; Zeng et al., 2023).

2.4.3 Sequential Gaussian simulation

The Sequential Gaussian simulation (SGS) method is a stochastic simulation approach that combines Gaussian probability with sequential simulation to generate spatial distribution of continuous variables, making it well-suited for handling such variables. Moreover, SGS is faithful to well data and considers simulated grid data during the simulation process. It is the most widely used method for property modeling (Karacan et al., 2012; Zhou et al., 2015).

3 Geological data analysis

3.1 Geological setting

The Qinshui Basin, situated in the middle of the North China Craton, possesses ample CBM resources. It is a faulted basin that emerged through the differential uplift of fault blocks following the coal-forming period in the late Paleozoic era in north China. The basin has experienced four stages of tectonic movements, namely the Hercynian, Indosinian, Yanshanian, and Himalayan orogenies. Under the influence of the Yanshanian stress field, the current tectonic framework exhibits a large compound syncline structure in the NNE direction (Cai et al., 2011). The depth of the coal reservoirs gradually increases from the edge of the basin into the core of the syncline. Buried depth of No. 15 coal reservoir is less than 400 m at the south-eastern basin margin and more than 2200 m in the central basin (Qin et al., 2018). Qinshui Basin, one of China's two major CBM industrial bases, boasts cumulative proven CBM resources exceeding 2800 × 10^8 m^3. Its CBM production in 2021 accounted for 73.2% of the country's total production during the same period (Men et al., 2022). Presently, CBM exploration and development primarily focus on the shallow coal reservoirs in the southern region of the basin. In recent years, progress has been made in the development of CBM at depths greater than 1200 m in blocks such as Shizhuangbei and Zhengzhuang (Liu et al., 2022b).

The Yushe-Wuxiang block is situated in the middle eastern region of the Qinshui Basin, covering an area of 1219.72 km^2 (Fig. 2). Influenced by regional tectonics, the study area generally exhibits a monoclinic structure with a NE-SW strike and NW dip. The dip angle of the strata is predominantly below 10°, with well-developed folds and faults. Successive deposition in the study area encompasses various strata from the Lower Paleozoic Cambrian and Ordovician to the Upper Paleozoic Carboniferous and Permian, followed by the Mesozoic Triassic and Jurassic, and finally the Cenozoic Paleogene, Neogene, and Quaternary formations. The primary coal-bearing strata within the study area are the Upper Carboniferous Shanxi Formation and the Lower Permian Taiyuan Formation, encompassing a total of 20 coal reservoirs. The Taiyuan Formation mainly develops barrier and offshore shelf sedimentary system composed of shale, sandstone, limestone and coal reservoir. The Shanxi Formation is deposited in the fluvial delta sedimentary system, mainly containing shale, sandstone and coal reservoir. Among these reservoirs, the No. 3 coal

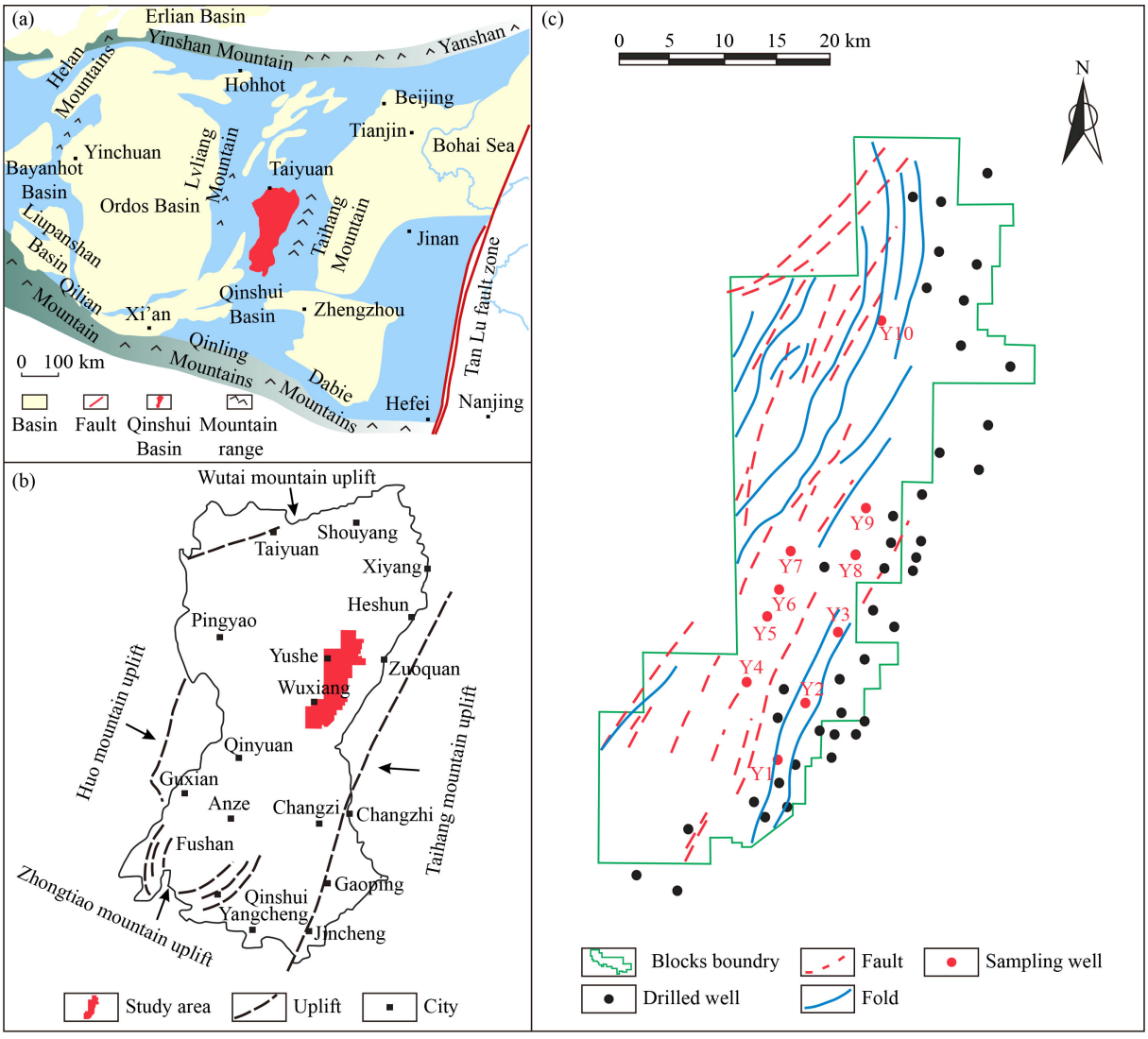

Fig. 2 Location of the Yushe-Wuxiang block and well distribution. (a) Location within the Qinshui basin; (b) location of the study area; (c) distribution of wells (modified from Li et al. (2018a); Jiang et al. (2023)).

reservoir of the Shanxi Formation and the No. 15 coal reservoir of the Taiyuan Formation have large burial depths and thicknesses, have great potential for deep CBM development (Su et al., 2018; Zhang et al., 2019; Hou et al., 2020; Xie et al., 2022).

3.2 Lithology identification based on logging normalization

Accurate lithology identification serves as the foundation for 3D geological modeling. Logging plays a crucial role in identifying lithology for non-core wells, providing essential data for stratigraphic division, correlation, and coal-bearing strata structure modeling. Moreover, the lithology of the coal reservoir roof and floor is a vital parameter in predicting favorable areas for CBM.

The accuracy of logging normalization is partially influenced by the selection of standard layers and standard wells. To optimize the process, well Y2 was selected as the standard well. Moreover, the K8 sandstone and No. 15 coal reservoir are identified as standard layers due to their substantial thickness, stable lateral distribution, distinctive logging response characteristics, and strong comparability. Taking the study area's DEN logging as an example, the histogram method is employed for normalization. After the normalization correction, both wells align with a main frequency range of 1.5−1.55 g/cm^3, resulting in a similar frequency distribution. This normalization effectively eliminates logging data errors (Fig. 3).

Utilizing the standardized logging data, an investigation is conducted to explore the relationship between lithology and electrical properties. The logging response characteristics of cored wells are analyzed to establish a lithology identification chart. Six lithologies are identified within the Benxi-Shanxi Formation in the study area: sandstone, mudstone, silty sandstone, coal, limestone and carbonaceous mudstone. These lithologies exhibit distinct

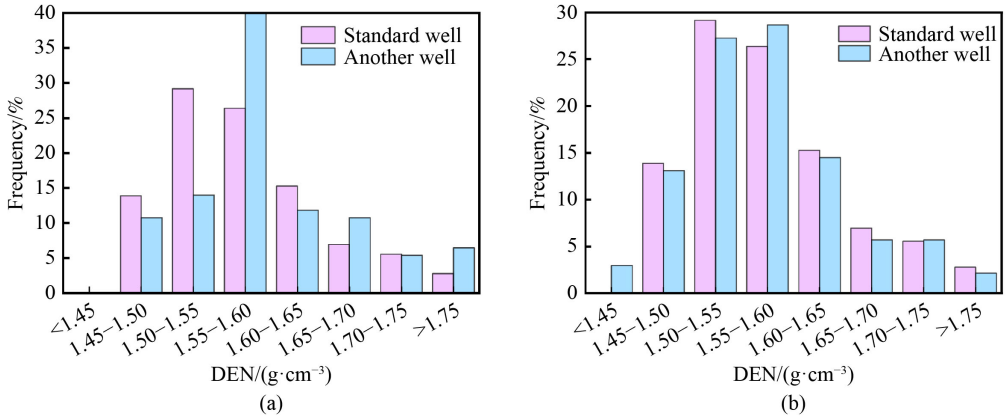

Fig. 3 DEN histogram before and after normalization of wells. (a) Before normalization of wells; (b) after normalization of wells.

logging response characteristics. To identify lithologies effectively, five logging parameters sensitive to lithology changes are selected for analysis: AC (acoustic), GR (gamma ray), DEN (density), CNL (compensated neutron), and RD (deep lateral resistivity). In the DEN-GR cross plot (Fig. 4), the six lithologies are distinguishable in different areas based on their respective logging values. The criteria for differentiation are as follows: coal (DEN < 1.8 g/cm^3), carbonaceous mudstone (1.8 < DEN < 2.1 g/cm^3), mudstone (DEN > 2.1 g/cm^3, GR > 134 API), silty sandstone (DEN > 2.2 g/cm^3, 106 < GR < 134 API), sandstone (DEN > 2.2 g/cm^3, 82 < GR < 106 API), and limestone (DEN > 2.7 g/cm^3, GR < 82 API).

The lithology identification chart providing a reliable means to identify the six lithologies present in the study area. This chart facilitates accurate lithology identification of non-core wells, offers insights into coal reservoir thickness, and determines the lithology of the roof and floor. Furthermore, it aids in identifying marker layers, thereby establishing a crucial data foundation for stratigraphic division, correlation, and 3D geological modeling.

3.3 Sequence stratigraphy division and correlation

The coal-bearing strata in the study area are characterized by marine-continental transition facies, where lithology with symbiotic relationships is regularly repeated and alternated. Vertically, multiple sets of thin coal reservoirs are present, and displaying features such as bifurcation, pinch-out, and merger. Therefore, the spatial distribution of the coal reservoirs remains uncertain, and the lithology of the coal reservoir roof and floor exhibits variability. The distribution and thickness changes of lithology are notably influenced by the sequence framework. Stratigraphy division and correlation are conducted within this isochronous sequence framework to solve the problems of poorly recognized coal reservoirs and cross-stratigraphy correlation in traditional studies. This approach serves as a critical foundation for 3D geological modeling of the coal-bearing strata. (Holz et al., 2002; Wang et al., 2019). Guided by the high-resolution sequence theory, this study conducts a comprehensive analysis of logging data, lithology and CWT. The key boundaries of the Benxi-Shanxi Formation sequence stratigraphy are determined, and stratigraphy division and correlation were made within the sequence framework (Fig. 5). Based on the outcomes of lithology identification, an analysis is conducted to examine the characteristics of vertical lithology cycle changes and identify key sequence interfaces. The lower sequence boundaries of SQI-SQIII are represented by the weathering crust at the top of the Ordovician, the bottom of the No. 15 coal reservoir, and the bottom of the K7 sandstone (Beichagou sandstone). These sequence boundaries exhibit significant characteristics, including a regional weathering unconformity surface, a transition surface indicating marine transgressive direction, and a sedimentary system transition surface. Notably, the maximum flooding surface is identified as the bottom surface of the K0 limestone (Bangou limestone), the bottom surface of the K3 limestone (Maoergou limestone), and the bottom surface of the No. 3 coal roof sandstone. At these key interfaces, distinctive logging response characteristics are evident. The GR logging demonstrates high values at the sequence interfaces and low values at the maximum flooding surface.

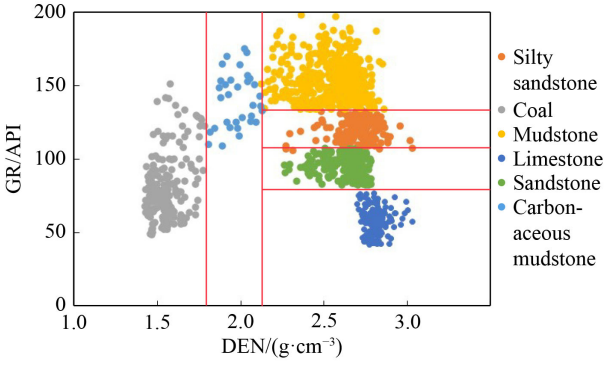

Fig. 4 Lithology identification chart of the study area.

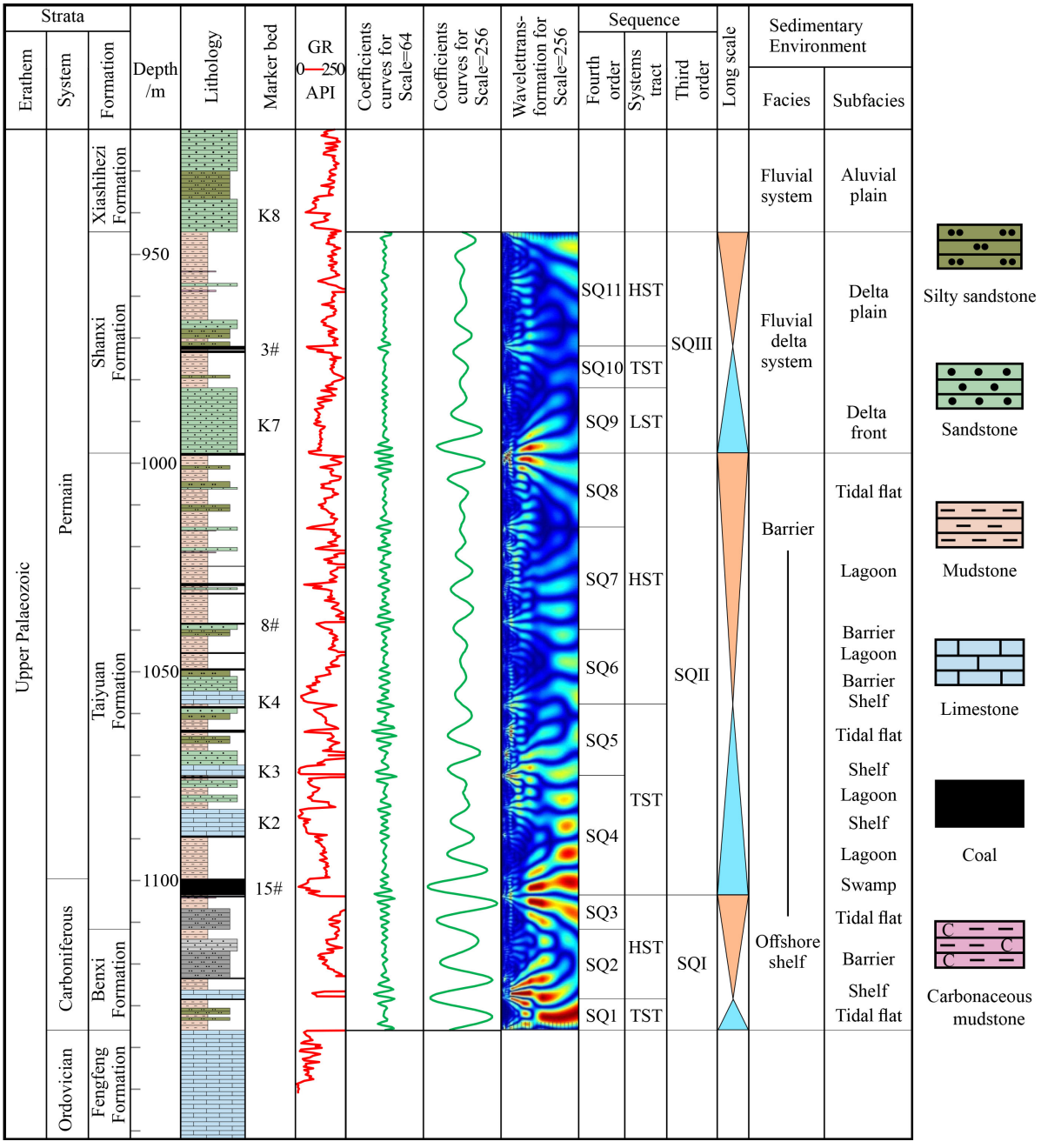

Fig. 5 Stratigraphy sequence identification and division of the Benxi-Shanxi Formation in the Yushe-Wuxiang block.

CWT is applied to analyze the standardized GR logging, resulting in the information of wavelet coefficient curves and wavelet transformation. The sequence boundary is associated with a large scale and strong energy within the energy group observed in the wavelet transformation. This is reflected in the violent oscillation and significant amplitude of the wavelet coefficient curve. Conversely, at the maximum flooding surface, the energy group in the wavelet transformation exhibits a smaller scale, resulting in gentle oscillations and a reduced amplitude in the wavelet coefficient curve (Fig. 5).

In the study area, the coal bearing strata of the Benxi-Shanxi Formation are classified into three third-order sequences and 11 fourth-order sequences (Fig. 5). Based on the single well sequence division of representative wells, the sequence stratigraphy framework is established through a comparative analysis of well profiles. A detailed stratigraphic correlation is conducted within the fourth-order sequence. According to the results from the lithology identification chart, specific marker layers are selected in a shallow-to-deep order, including K8 sandstone, No. 3 coal reservoir, No. 8 coal reservoir, K4 limestone, K2 limestone, No. 15 coal reservoir, and the mudstone section at the bottom of the Benxi Formation.

These marker layers are employed to facilitate stratigraphic correlation, elucidating the distribution patterns of coal reservoirs. Thick coal reservoirs primarily exhibit distribution within the ascending half cycle of the third-order sequence. The No. 15 coal reservoir was formed in a sedimentary environment characterized by a barrier-offshore shelf near the sea. It is positioned in the lower section of the transgressive system tract (TST) within the third-order sequence SQII. Moreover, it resides within the fourth-order sequence SQ4. Conversely, the No. 3 coal reservoir was formed in a shallow water fluvial delta sedimentary environment on the land side. It is situated in the middle and upper portions of the transgressive system tract (TST) within the third-order sequence SQIII. Additionally, it is located within the fourth-order sequence SQ10 (Fig. 6).

By considering the correlation results of the marker layers within the isochronous sequence framework, the accuracy of stratigraphy division and correlation is ensured. This process further facilitates the clarification of the distribution patterns of coal reservoirs. In particular, the seven identified marker layers serve as the foundational basis for establishing the layer surface model in subsequent structural modeling endeavors.

3.4 Fine structural interpretation

Fine structural interpretation was conducted using the well-seismic combination methods, and the results showed that there are a total of 29 faults developed in the study area, consisting of 22 normal faults and 7 reverse faults. These faults generally strike NNE-NE, with an average azimuth of 60°NE and a dip toward NWW. Their extension lengths vary, with some reaching up to 20 km, and the amount of displacement ranges from 20 to 165 m. Overall, fault development in the study area is characterized by a greater concentration in the west, and a lesser occurrence in the east. In the middle south of the study area, a conical collapse column is present, affecting the coal-bearing strata of the Benxi-Shanxi Formation and covering an area of 500 m in diameter.

Utilizing the fault data from structural interpretation, the faults are imported into the Petrel. Subsequently, the faults from different surfaces are classified, which are used to analyze the vertical extension length and dip angle. After the initial fault model is established, the 3D visual interactive window is used to modify the model according to the fault relationship. Subsequently, the fault model is established, ensuring the rational representation

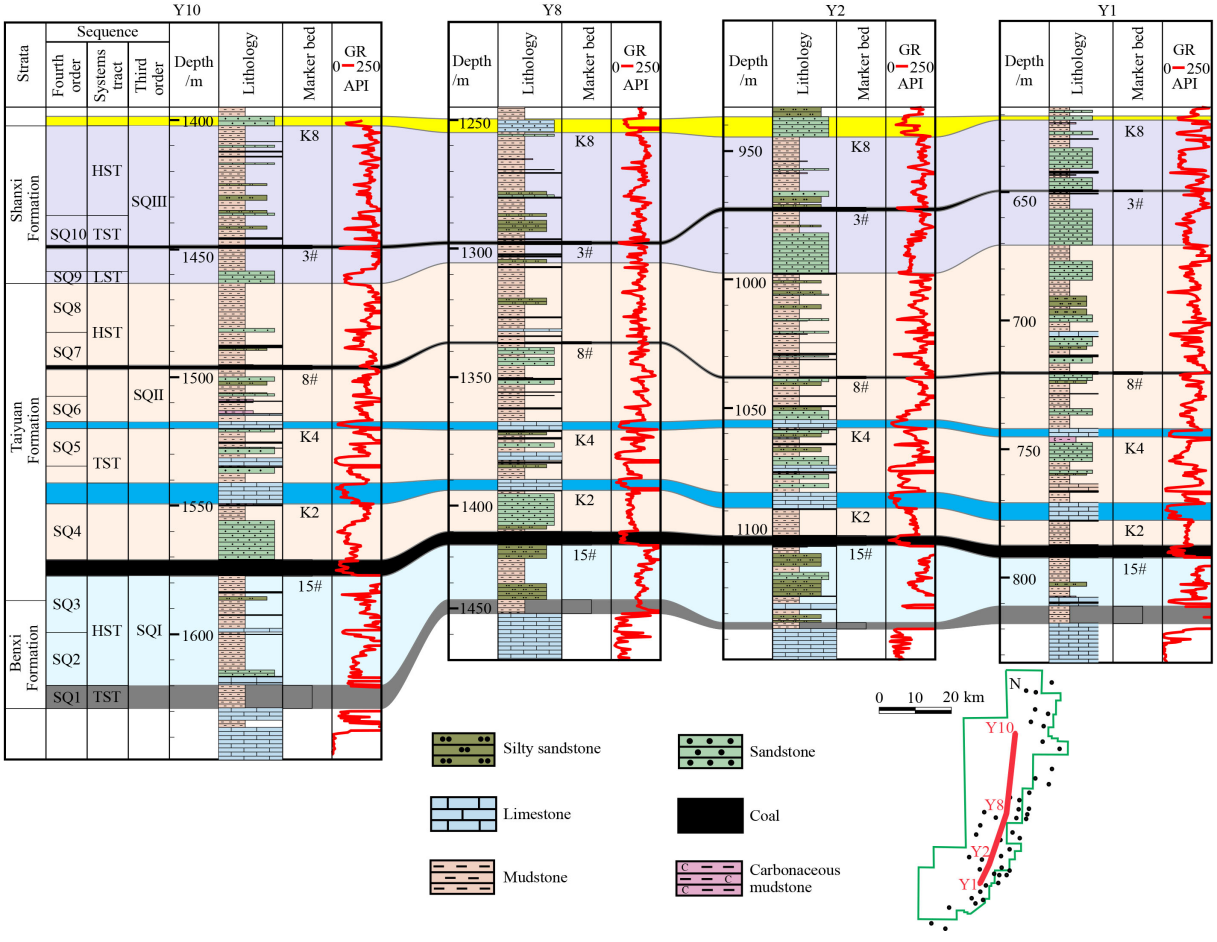

Fig. 6 Stratigraphy correlation of the Benxi-Shanxi Formation in the Yushe-Wuxiang block.

of fault characteristics and their distribution.

4 3D geological modeling

3D geological modeling involves the utilization of a model to depict the distribution and variations of reservoir structure and properties in three-dimensional space. The primary objective is to predict reservoir parameters between wells (Liu et al., 2022c). In this study, Petrel is employed as the modeling platform, combining deterministic modeling and stochastic modeling approaches to progressively construct a coal reservoir structure model, facies model, and property model within the study area.

4.1 Structural modeling

A structural model provides insights into the fundamental spatial distribution characteristics of the reservoir, encompassing the fault model, layer surface model, and grid design (Zhou et al., 2012). It serves as a crucial foundation for subsequent facies modeling and property modeling. Only when facies and property models are established upon precise and reliable structural models can they be better aligned with actual reservoir conditions.

To account for the modeling area, well distribution, and calculation precision, the grid step size on the plane is set at 100 m × 100 m, extending along 60°NE. Vertically, based on the identification of 7 marker layers through stratigraphy division and correlation, the coal-bearing strata of the Benxi-Shanxi Formation are divided into 12 smaller layers. Moreover, the target coal reservoir is further subdivided into 5 layers. This results in a total of 231344 single-layer grids, 3470160 grids for the coal reservoir, and 5552256 grids for the entire Benxi-Shanxi Formation structural model.

The structural modeling process follows the 'point-surface-volume' approach. It is based on the stratigraphy correlation outcomes derived from drilling data within the isochronous sequence framework and is further constrained by the detailed interpretation results of seismic data structures. Seven layers models were established, encompassing K8 sandstone, No. 3 coal reservoir, No. 8 coal reservoir, K4 limestone, K2 limestone, No. 15 coal reservoir, and the mudstone section at the bottom of the Benxi Formation. These layer models are overlaid with the fault model, and through the deterministic modeling method, a structural model reflecting the spatial variation characteristics of strata is established using Kriging interpolation (Fig. 7).

The strata within the study area exhibit a pattern of higher elevation in the east and lower elevation in the west. The north-west and south-east regions are influenced by intense tectonic activities, resulting in relatively developed faults and folds, leading to undulating strata. Various sections are intercepted in different directions to analyze the structural characteristics of each section and its impact on reservoir distribution. In the east–west section (Fig. 8(a)), the overall strata fluctuation is significant, displaying the characteristics of higher elevation in the east and lower elevation in the west. In the north-west part of the section, a structural formation of two anticlines and one syncline is observed. The presence of faults DF17, DF18, DF20, DF21, and DF16 significantly affects the distribution of coal reservoirs, causing notable breaks between the upper and lower plates. In contrast, the north–south section (Fig. 8(b)) shows a gentler fluctuation of the stratigraphy, with the feature of lower elevation in the north-east and higher elevation in the south-west. Fault displacement is relatively short, and there is development of folds. Consequently, the distribution of coal reservoirs is stable, and their continuity is relatively robust.

The structural model of the coal reservoir accurately reflects the spatial framework of the CBM reservoir in the study area, providing an accurate description of the distribution and variation characteristics of the coal reservoir. The thickness of the No. 3 coal reservoir ranges from 0 to 2.19 m, with an average thickness of 1.09 m. The thickest region is found in the middle of the study area, and the overall buried depth varies from 284 to 2000 m. On the other hand, the No. 15 coal reservoir exhibits a relatively large thickness, ranging from 1.12 to 6.3 m,

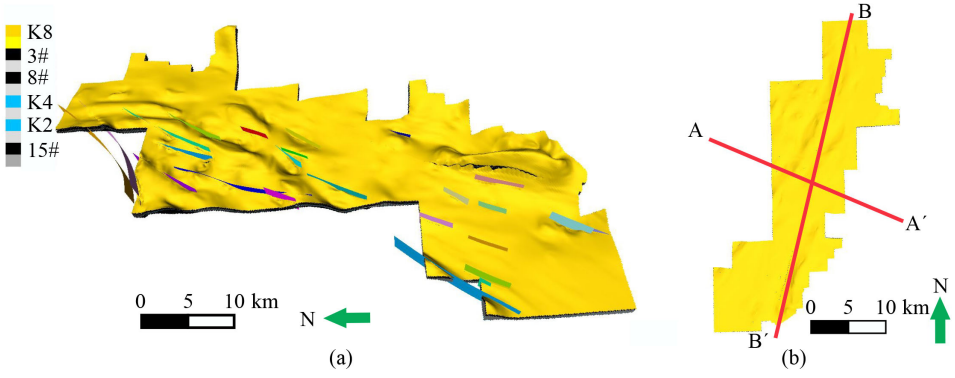

Fig. 7 Stratigraphy structure model and section location map of the Benxi-Shanxi Formation in the study area.

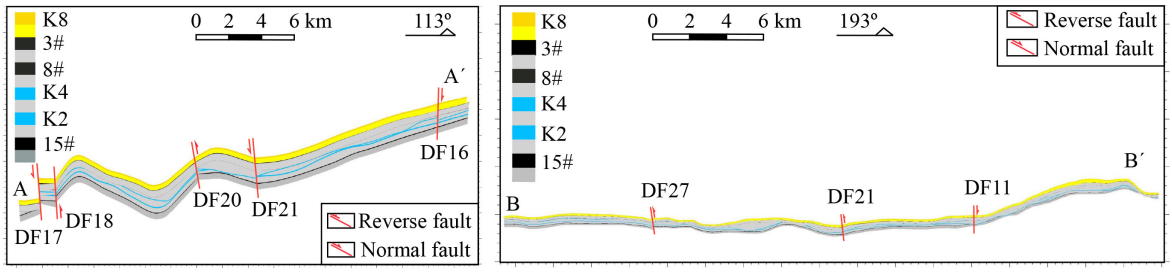

Fig. 8 Cross-section view of the coal-bearing stratigraphy structure model of the Benxi-Shanxi Formation in the study area. (a) A–A′ profile; (b) B–B′ profile.

with an average thickness of 4.45 m. The western part of the study area contains the thickest sections, and the overall buried depth varies from 399 to 2000 m. Moving from south-east to north-west, the buried depth of both coal reservoirs gradually increases, and the south-east region experiences lower continuity due to the influence of faults (Fig. 9).

4.2 Facies modeling

In 3D geological modeling of conventional oil and gas reservoirs, facies modeling involves establishing sedimentary facies or lithofacies models as constraints for property models, followed by facies-controlled property modeling (Ren et al., 2019). Coal reservoir exhibit significance heterogeneity, and there are great differences in porosity, permeability, gas content, gas occurrence state and gas output characteristics of coal with different coal body structure. The coal body structure plays a vital role in influencing reservoir properties, which, in turn, affects reservoir productivity and recoverability. Therefore, it is of great significance to carry out the research on the modeling of coal body structure facies for the establishment of subsequent coal reservoir property model and the understanding of CBM enrichment law. Different coal body structures can be classified into four types based on the degree of coal deformation: undeformed, cataclastic, granulated, and mylonitized (Fu et al., 2009). These varying structures exhibit different properties, resulting in distinct logging response characteristics. Previous studies have summarized the logging response characteristics of different coal body structures in the adjacent regions of the Qinshui Basin. The AC, GR, RD, and DEN logging values show a strong correlation with the coal body structure. As the degree of coal deformation increases, the AC and RD logging values tend to increase, while the GR and DEN logging values decrease (Fig. 10) (Teng et al., 2015; Li et al., 2021).

Considering the deformation degree of coal samples in the study area and previous research findings, the coal body structure is classified into three types labeled I, II, and III, representing undeformed, cataclastic, and granulated-mylonitized structures, respectively. To quantitatively identify the coal body structure at individual wells, the standardized logging data of AC, GR, RD, and DEN were employed (Fig. 11). The coal body structure in the research area heavily relies on well data, as seismic data may not effectively reflect its characteristics. Additionally, the limited number of wells and considerable spacing between them make it challenging to accurately simulate using deterministic modeling interpolation methods. As a result, stochastic simulation methods prove more suitable for this purpose. The coal body structure in the study area is a discrete variable, exhibiting significant heterogeneity. To effectively model this variability, the sequential indicator simulation (SIS) method is used for coal body structure modeling. After encoding the three types of coal body structure, the variation function is analyzed and established to create coal body structure models for both the No. 3 coal reservoir and No. 15 coal reservoir (Fig. 12).

Based on Fig. 12, it is evident that the coal body structure of the Nos. 3 and 15 coal reservoirs in the study area is predominantly type I, with localized development of type II in the central region and more extensive presence of type II and III in the south-east. Overall, the coal body structure exhibits relative completeness, making it suitable for hydraulic fracturing reservoir

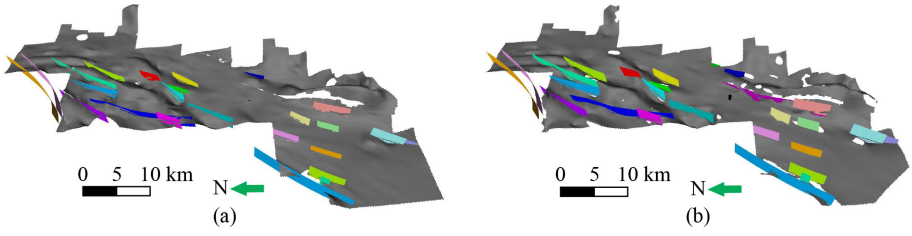

Fig. 9 Structure model of the coal reservoir in the study area. (a) No. 3 coal; (b) No. 15 coal.

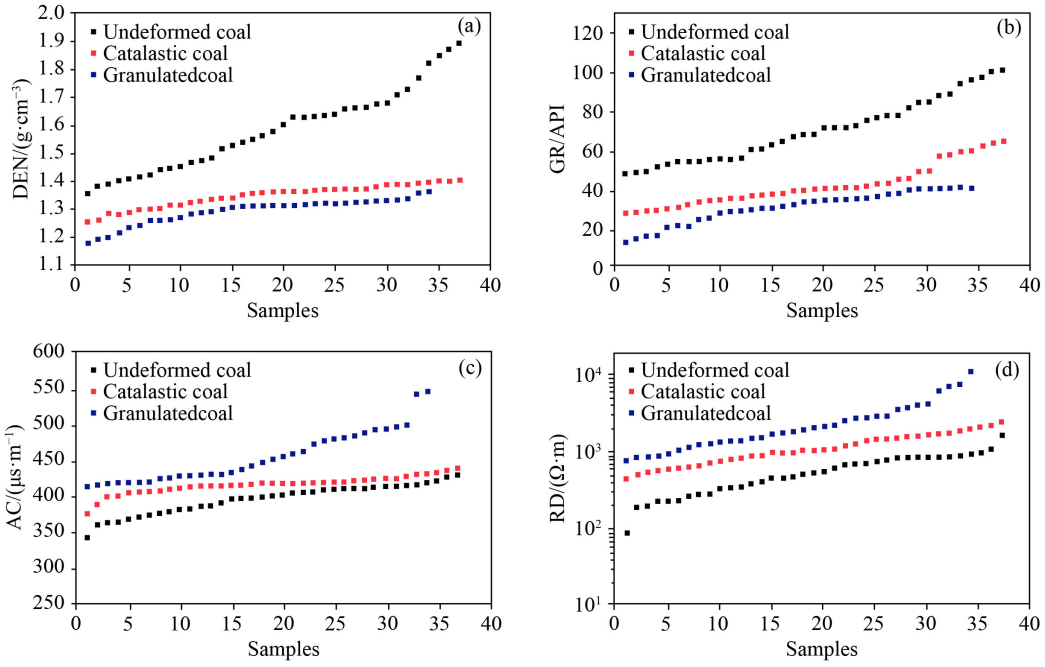

Fig. 10 Logging data of coal with different coal body structures. (a) DEN; (b) GR; (c) AC; and (d) RD (modified from Teng et al. (2015)).

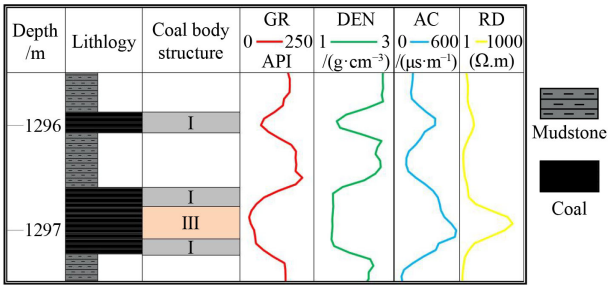

Fig. 11 Logging data and coal body structures identification results of well Y8.

reformation during later development stages. The occurrence of type II and type III is linked to tectonic conditions, primarily concentrated in the fault-intensive area and fold core in the south-eastern part of the study area, indicating the disruptive impact of tectonic movement on coal reservoirs. Specifically, the No. 3 coal reservoir is significantly influenced by tectonic action, leading to a higher prevalence of type III.

4.3 Property modeling

The primary objective of 3D geological modeling of coal reservoirs is to create a property model that accurately represents the distribution and variations of coal reservoir property parameters in the study area. It focuses on both the prediction of unknown areas between wells and the quantified characterization of reservoir heterogeneity. This is the central aspect of 3D geological modeling and encompasses important parameters such as gas content, permeability, and porosity. To precisely characterize these coal reservoir properties, various tests were conducted on core samples as detailed in Table 1. All experimental tests adhered to national standards and relevant specifications, and were carried out in certified laboratories without encountering any abnormal conditions.

These property parameters of coal reservoirs are all continuous variables, and the SGS is selected for property modeling. Variogram is a fundamental tool in geostatistics used to characterize the stochastic and spatial correlation of regionalized variables. It is an important

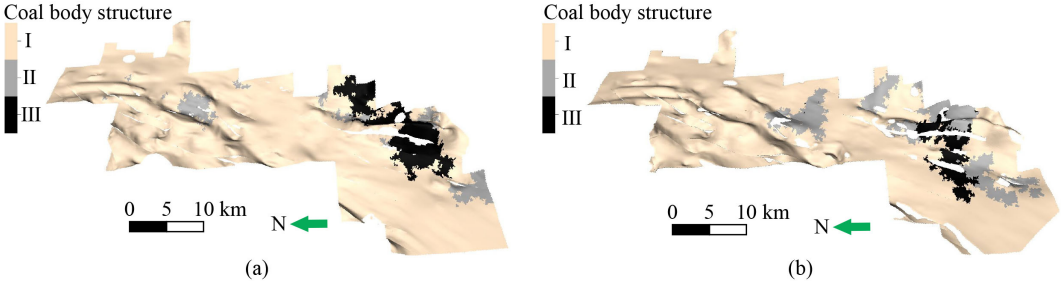

Fig. 12 Coal body structure models of coal reservoirs in the study area. (a) No. 3 coal; (b) No. 15 coal.

Table 1 Analyzed samples and the applied measurements

Property parameters	Measurements	The number of measured samples	
		No. 3 coal	No. 15 coal
Gas content	Canister desorption	11	13
	Isothermal adsorption	11	11
Porosity	High-pressure mercury intrusion	12	12
	Low-temperature liquid nitrogen adsorption	4	4
Permeability	Well testing	2	2

factor that influences the accuracy of stochastic modeling (Liu et al., 2022c). Considering the analysis of regional sedimentary environments, the provenance directions of the Shanxi and Taiyuan formations are north-east and north, respectively. Therefore, for the variogram of No. 3 coal, the major range directions were set as north-east, and for the variogram of No. 15 coal, the major range directions were set as north. The lag distance and search radius were determined based on the analysis of well spacing in the study area (Fig. 1). The sedimentary environment of both No. 3 and No. 15 coal reservoirs is relatively stable, which led to the selection of a spherical model to match the variogram (Guo et al., 2015; Liu et al., 2023). Table 2 presents the calculation results of the variogram, including the range, fitting type, still, and nugget. Based on the structural model and using the coal body structure model as a constraint, the SGS method was chosen for stochastic simulation through grid coarsening, variogram setting, and other steps. Finally, separate gas content, porosity, and permeability models were established for the Nos. 3 and 15 coal reservoirs in the study area.

4.3.1 Gas content

Based on the direct gas desorption measurement data from the Nos. 3 and 15 coal reservoirs in the study area, a gas content model was established (Figs. 13(a) and 13(b)). The gas content of the No. 3 coal reservoir ranges between 12.21 to 28.67 $m^3 \cdot t^{-1}$, with an average of 17.03 $m^3 \cdot t^{-1}$. The areas with high gas content are located in the north-west and south-west. For the No. 15 coal reservoir, the gas content ranges between 9.33 to 23.28 $m^3 \cdot t^{-1}$, with an average of 17.59 $m^3 \cdot t^{-1}$, slightly higher than that of the No. 3 coal reservoir. The high gas-bearing areas are found in the north and south-west.

In the study area, the correlation between the gas content of coal reservoirs and coal body structure is relatively weak, while the correlation with burial depth is strong. Generally, the gas content of the Nos. 3 and 15 coal reservoirs increases with the burial depth. The gas content is notably higher in the western part due to its greater burial depth, while the south-east exhibits lower gas content due to the combined adverse factors of shallow burial depth and complex structure.

4.3.2 Porosity

The pore characteristics of coal reservoirs were analyzed through high-pressure mercury intrusion and low-temperature liquid nitrogen adsorption experiments, using a decimal classification (micropore, < 10 nm; transition pore, 10−100 nm; mesopore, > 100 nm; macro-pore, > 1000 nm) (Xu et al., 2019). In the study area, the Nos. 3 and 15 coal reservoirs show the most developed transition pore, followed by micropores. Generally, open-type pores are predominant in both coal reservoirs, with some pores having one end sealed. The porosity of the coal reservoirs, obtained through high-pressure mercury injection experiments, reveals interesting trends. For the No.3 coal reservoir, the porosity ranges between 0.27% to 18.72%, with an average of 6.1%. High porosity areas are observed in the north and south-east of the block. On the other hand, the No. 15 coal reservoir displays porosity levels ranging from 1.76% to 27.7%, with an average of 11.5%. Notably, the porosity of No. 15 coal reservoir is

Table 2 Variogram settings for the coal

Coal	Property	Major range/ m	Minor range/ m	Vertical range/ m	Azimuth/ (°)	Fitting type	Still/ m^2	Nugget
No. 3	Gas content	14,187	7541	/	225	spherical	1	0.155
	Porosity	7437	4503	/	225	spherical	1	0.121
	Permeability	15,352	6002	/	225	spherical	1	0
No. 15	Gas content	12,490	8209	/	180	spherical	1	0.125
	Porosity	7912	4003	/	180	spherical	1	0.0075
	Permeability	6465	4002	/	180	spherical	1	0

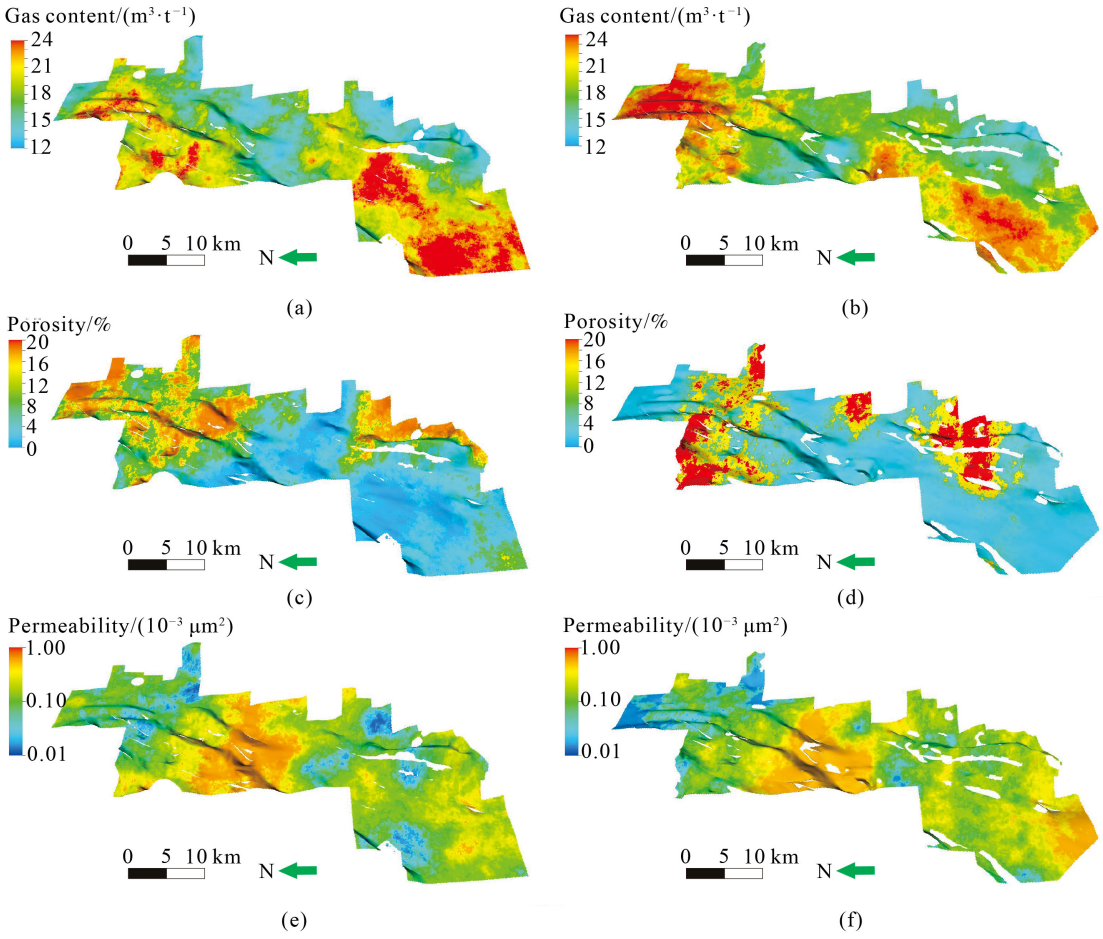

Fig. 13 Property models of coal reservoirs in the study area. (a), (c), (e), No. 3 coal; (b), (d), (f), No. 15 coal.

significantly higher than that of No. 3 coal reservoir, and the porosity is relatively higher in the north and southeast of the block (Figs. 13(c) and 13(d)).

As the degree of coal damage increases, there is a clear trend of increasing porosity in the coal reservoirs. Specifically, the porosity follows the sequence of type III > type II > type I, with type III exhibiting the highest porosity due to the development of pores of different sizes, especially mesopores and macropores, which significantly contribute to the overall porosity. In the western part of the study area, the coal reservoirs are buried at depths greater than 1500 m, experiencing high in situ stress conditions. Consequently, the pores and fissures tend to close, leading to a significant decrease in porosity.

4.3.3 Permeability

In the study area, only two wells have undergone permeability testing, resulting in significant differences in permeability values and limited data availability. Therefore, the permeability of the coal reservoir is predicted using the Timur formula (Shi et al., 2020). The permeability of coal reservoirs in 14 wells was calculated using the Timur formula. As shown in Figs. 13(e) and 13(f), the average permeability of the No. 3 coal reservoir is estimated to be 0.18×10^{-3} μm², while the average permeability of the No. 15 coal reservoir is calculated to be 0.25×10^{-3} μm². Overall, most of the coal reservoirs in the study area exhibit permeabilities less than 0.5×10^{-3} μm², indicating low permeability characteristics. However, there is a relatively high permeability zone located in the middle of the block:

$$K = 0.136 \times \phi_e^{4.4} / S_{wi}^2, \tag{4}$$

where K is the permeability in 10^{-3} μm², ϕ_e represents the porosity in %, S_{wi} is the bound water saturation in %.

Coal body structure is a significant controlling factor of permeability in the study area. The permeability of coal reservoirs follows a trend of initially increasing and then decreasing with the degree of coal deformation. Type II coal reservoirs exhibit the highest permeability, followed by type I, while type III has the lowest permeability. This variation can be attributed to the impact of coal deformation on the natural fracture system. Type II coal, undergoing brittle deformation or failure due to weak tectonic stress, forms new fractures that serve as fluid flow channels, enhancing permeability. In type III coal,

the impact of strong tectonic stress leads to deformation and destruction of the natural fracture system, causing coal powder filling, which results in reduced permeability.

4.4 Model verification

After completing the 3D geological modeling, it is essential to test the model's compliance with geological knowledge and verify its accuracy, considering the inherent stochastic nature and uncertainties involved. To achieve this, the principle of 'probability distribution consistency' is employed in this study for model verification (Leuangthong et al., 2004). This verification process involves drawing frequency distribution histograms and comparing the input data, upscaled data, and simulated data to ensure consistency. By quantitatively verifying the model against the actual data, the accuracy and reliability of the established model can be assessed.

Using the gas content model of the No. 15 coal reservoir as an example, the frequencies of the three data sets are similar, and the error is less than 5% (Fig. 14). The established property model effectively reflects the distribution characteristics of the input data, aligning with the actual conditions, thus confirming the accuracy and reliability of the 3D geological model.

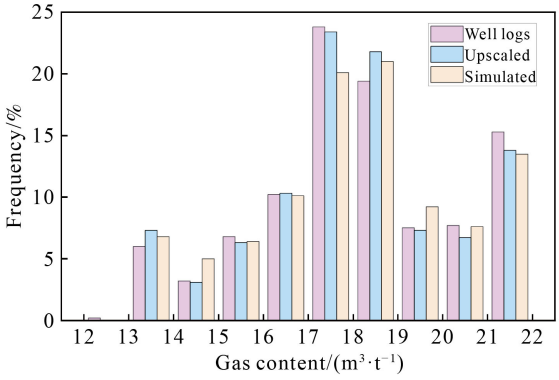

Fig. 14 Statistical and histogram analysis to compare input gas content logs with simulated gas content.

5 Application of the model

5.1 Estimation of CBM resources

The estimation methods for CBM resources encompass various approaches, such as the volumetric method, analogy method, and production decline method, among others (Altowilib et al., 2020). Due to the early stage of development and the lack of production dynamic data for the CBM reservoir in the study area, the resources estimation relies on the volumetric method, which utilizes static data. Leveraging the 3D geological model that has been established, the 'volume calculation' module in Petrel is employed to calculate the CBM resources in each grid. The CBM resources in the Yushe-Wuxiang block are determined using the following equation:

$$G = \sum V_{\text{Bulk}} \cdot \rho \cdot F, \tag{5}$$

where G is the gas volume in m^3, V_{Bulk} represents the volume of grids in m^3, ρ is the coal density in g/cm^3, and F denotes the gas content in $m^3 \cdot t^{-1}$.

Having more realizations can provide a better representation of the uncertainty in subsurface parameter distribution. One hundred stochastic models were created, and the CBM resources were calculated for each of these models. As shown in Fig. 15, P90, P50, and P10, representing low, medium, and high probability resources, respectively, are determined by drawing frequency and cumulative probability distribution diagrams.

The calculated CBM resources of the No. 3 coal at the P90, P50, and P10 levels of confidence are 483.78 × 10^8 m^3, 487.64 × 10^8 m^3, and 491.31 × 10^8 m^3, respectively. The calculated CBM resources of the No. 15 coal at the P90, P50, and P10 levels of confidence are 1949.38 ×

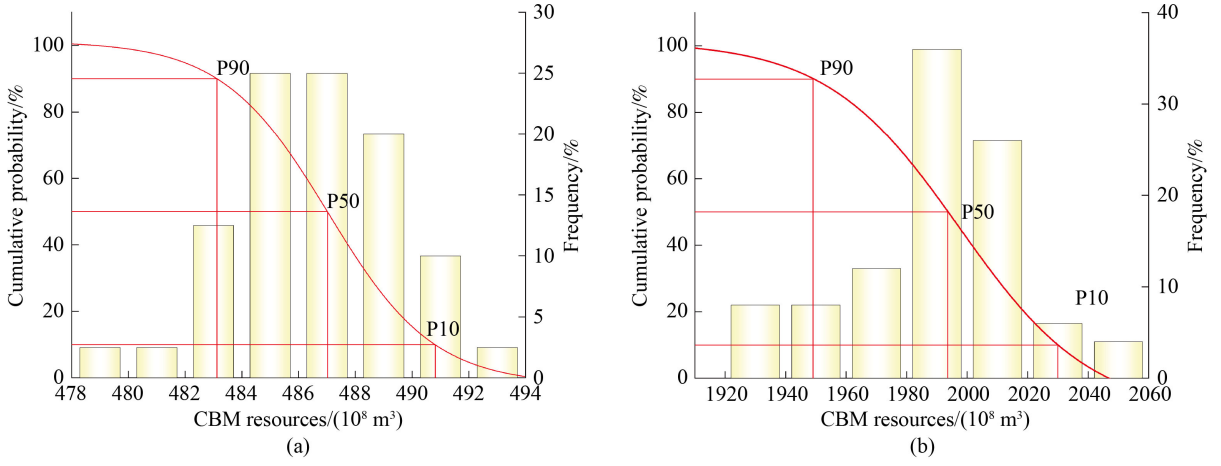

Fig. 15 Probabilistic CBM resource diagrams. (a) No. 3 coal; (b) No. 15 coal.

10^8 m^3, 1993.66 × 10^8, m^3 and 2030 × 10^8 m^3, respectively. The P50 estimate represents the most likely CBM resource quantity, and it is the most probable CBM resource estimate at the P50 confidence level. The integrated analysis indicates that the total amount of CBM resources in both the No. 3 coal reservoir and the No. 15 coal reservoir in the study area is 2481.3 × 10^8 m^3, classified as a large CBM gas field.

5.2 Favorable area prediction

After a comprehensive analysis of CBM enrichment and accumulation factors in the study area, resource conditions, reservoir properties, and preservation conditions are identified as the primary controlling factors of CBM enrichment. Quantitative evaluation indexes such as coal reservoir thickness, gas content, porosity, permeability, and burial depth are selected, along with qualitative evaluation indexes including coal body structure, roof-floor lithology, and structural complexity (Table 3) (Yao et al., 2009; Wang et al., 2018). To integrate these factors effectively, a combination of hierarchical analysis and the fuzzy mathematics method, known as the multi-level fuzzy method, is applied. This approach enables the conversion of contradictory, qualitative, and quantitative geological factors into compatible geological factors through specific calculations, facilitating the determination of evaluation scores to scientifically assess the CBM potential and predict favorable areas (Table 4).

As depicted in Fig. 16, the study area is divided into subareas of four types based on the evaluation score, type I to type IV with descending evaluated scores. Type I is the most favorable area, with a score of > 0.6. Type II is a moderately favorable area with a score of 0.5−0.6. The favorable area for CBM in the No. 3 coal reservoir is primarily situated in the central and northern parts of the block. Conversely, the favorable area for CBM in the No. 15 coal reservoir is concentrated in the eastern and north-eastern regions of the block. These identified favorable areas are crucial for determining the optimal locations for future well deployments.

Based on the analysis, the CBM favorable area in the study region is mainly influenced by resource conditions, with the thickness of the coal reservoir and gas content being the main controlling factors affecting the CBM development potential. In the type I favorable area, the No. 15 coal reservoir generally exhibits a thickness greater than 5 m and a gas content higher than 18 $m^3 \cdot t^{-1}$. In the south-western region, the No. 15 coal reservoir demonstrates high permeability, favorable coal body structure, and minimal faults and folds, indicating good reservoir properties and preservation conditions. However, the coal reservoir thickness is less than 3 m, leading to poor resource conditions, which classifies them as type II favorable areas. The south-eastern part, characterized by developed folds and faults, experiences significant damage to the coal reservoir due to strong tectonic action, resulting in low gas content. In addition, the development of granulated-mylonitized coal under strong tectonic action is not conducive to reservoir fracturing and transformation. Hence, both structural complexity and coal body structure significantly impact the CBM development potential, and the south-eastern region exhibits lower potential due to unfavorable conditions.

5.3 The strengths of the workflow

Currently, deep CBM exploration is still in its early stages, and the low well spacing density and pronounced heterogeneity pose challenges for reservoir characterization and favorable area prediction. The limited quantity and distribution of available samples constrain the precision of these studies, rendering conventional methods insufficient for directly guiding CBM exploration. Well logging can be employed to estimate the reservoir properties of individual wells; however, this approach only provides localized information and is challenging to represent regional and spatial heterogeneity. When considering inter-well reservoir property, inter-well prediction requires the creation of multiple well-connected correlation profiles. This process is both time-consuming and labor-intensive, and inter-well prediction is often considered subjective. Although seismic response characteristics can offer valuable insights into inter-well reservoir property, this method is often constrained by the high-quality requirements and relatively low resolution of

Table 3 Evaluation parameters and their respective weights for identifying the CBM favorable zones in the study area

Evaluation object	Second-grade indicators	Weight	Third-grade indictors	Weight
A division of CBM favorable area	Resource conditions	0.47	Thickness of coal reservoir	0.315
			Gas content	0.155
	Reservoir properties	0.16	Coal body structure	0.04
			Permeability	0.08
			Porosity	0.04
	Preservation conditions	0.37	Roof-floor lithology	0.074
			Structural complexity	0.148
			Burial depth	0.148

Table 4 Evaluation standard and membership function for favorable areas of CBM

Item Parameter		Evaluation standard	Membership function
Resource conditions	Coal thickness/m	⩽ 0.5	0.1
		(0.5,2]	0.4M−0.1
		(2,5)	0.1M+0.5
		⩾ 5	1
	Gas content/($m^3 \cdot t^{-1}$)	⩽ 8	0.1
		(8,20)	0.075F−0.5
		⩾ 20	1
Reservoir properties	Coal body structure	I	0.8
		II	0.5
		III	0.2
	Permeability/(10^{-3} μm^2)	⩾ 0.5	1
		(0.25,0.5)	2.8K−0.4
		⩽ 0.25	0.3
	Porosity/%	⩽ 3	0
		(3,10)	0.1X
		⩾ 10	1
Preservation conditions	Roof-floor lithology	Mudstone/Carbonaceous mudstone	0.8
		Silty sandstone	0.5
		Sandstone/limestone	0.2
	Structural complexity	Simple structure with less fault	0.8
		Medium complexity structure	0.5
		Complicated structure with few fault	0.2
	Burial depth/m	⩽ 1000	(H−300)/700
		(1000,1500)	(1300−0.8H)/500
		⩾ 1500	0.2

seismic data in many cases.

In contrast, the 3D geological modeling workflow proposed in this article integrates logging, seismic, drilling, and testing data, which has significant advantages over traditional reservoir characterization methods. Through the analysis of multi-source geological data, it provides geological constraints for 3D geological modeling, minimizing its uncertainty. 3D geological modeling uses stochastic modeling methods to predict inter-well reservoir properties, guided by geostatistical results and geological understanding, which can effectively reduce subjectivity and solve the problem of low accuracy in traditional linear interpolation methods. Reliable geological models enable fine characterization of coal reservoirs, overcoming the limitations of sample quantity and location in regions with moderate to low exploration levels. The application of models can improve the accuracy of resource estimation and favorable area prediction, ensuring the scientific and rationality of the results. At the same time, the geological model is the foundation for later geological-oriented drilling, which is of great significance for the integration of geology-engineering integration, and can also be used for numerical simulation of CBM, ultimately achieving more efficient and sustainable exploration and development.

6 Conclusions

Accurately characterizing coal reservoirs and predicting favorable areas for CBM is a challenging work. This article highlights the potential of 3D geological modeling in CBM and presents a workflow applied to deep CBM resource evaluation. The following conclusions can be drawn.

1) Through the integration of multi-source geological data for comprehensive analysis, it provides geological constraints for 3D geologic modeling, which helps to reduce the uncertainty resulting from the low well networks density and significant reservoir heterogeneity in deep coal reservoir.

2) The establishment of structural models, facies models, and property models through 3D geological modeling methods grounded in geostatistics can enhance

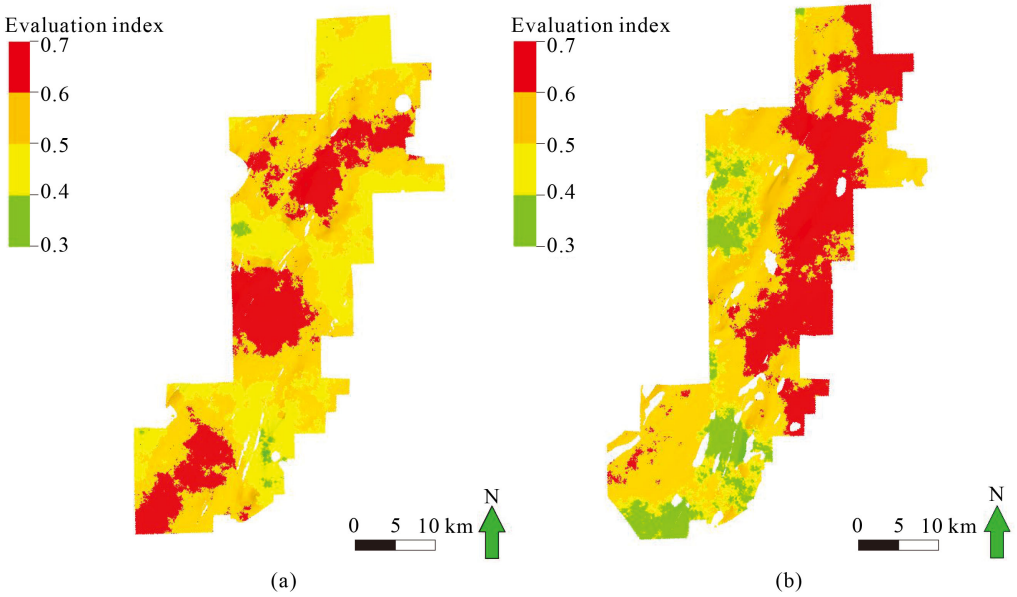

Fig. 16 Prediction map of CBM favorable zones in the study area. (a) No. 3 coal; (b) No. 15 coal.

the precision of inter-well parameter prediction and address the issue of inadequate prediction accuracy in conventional approaches.

3) Based on the 3D geological model, the CBM resources and favorable areas in Yushe-Wuxiang Block are predicted. This method improves CBM resource assessments and has the potential to be applied in other deep CBM blocks with moderate to low exploration levels.

Acknowledgments This research is funded by the NSFC-Shanxi Coal-based Low Carbon Joint Fund of China (No. U1910205), the National Natural Science Foundation of China (Grant No. 42272197).

References

Ali A M, Radwan A E, Abd El-Gawad E A, Abdel-Latief A S A (2022). 3D integrated structural, facies and petrophysical static modeling approach for complex sandstone reservoirs: a case study from the Coniacian-Santonian Matulla Formation, July Oilfield, Gulf of Suez, Egypt. Nat Resour Res, 31(1): 385–413

Altowilib A, AlSaihati A, Alhamood H, Alafnan S, Alarifi S (2020). Reserves estimation for coalbed methane reservoirs: a review. Sustainability (Basel), 12(24): 10621

Cai Y D, Liu D M, Yao Y B, Li J G, Qiu Y K (2011). Geological controls on prediction of coalbed methane of No. 3 coal seam in southern Qinshui Basin, north China. Int J Coal Geol, 88: 101–112

Duan L J, Qu L C, Xia Z H, Liu L L, Wang J J (2020). Stochastic modeling for estimating coalbed methane resources. Energy Fuels, 34(5): 5196–5204

Flores R M (2014). Coal and Coalbed Gas: Fueling the Future. Amsterdam: Elsevier

Fu X, Qin Y, Wang G G X, Rudolph V (2009). Evaluation of coal structure and permeability with the aid of geophysical logging technology. Fuel, 88(11): 2278–2285

Holz M, Kalkreuth W, Banerjee I (2002). Sequence stratigraphy of paralic coal-bearing strata: an overview. Int J Coal Geol, 48(3−4): 147–179

Hou X W, Liu S M, Zhu Y M, Yang Y (2020). Evaluation of gas contents for a multi-seam deep coalbed methane reservoir and their geological controls: in situ direct method versus indirect method. Fuel, 265: 116917

Hu L Y, Chugunova T (2008). Multiple-point geostatistics for modeling subsurface heterogeneity: a comprehensive review. Water Resour Res, 44(11): W11413

Guo Z, Sun L D, Jia A L, Lu T (2015). 3-D geological modeling for tight sand gas reservoir of braided river facies. Pet Explor Dev, 42(1): 83–91

Jiang F J, Jia C Z, Pang X Q, Jiang L, Zhang C L, Ma X Z, Qi Z G, Chen J Q, Pang H, Hu T, Chen D X (2023). Upper Paleozoic total petroleum system and geological model of natural gas enrichment in Ordos Basin, NW China. Pet Explor Dev, 50(2): 281–292

Kadkhodaie A, Rezaee R (2017). Intelligent sequence stratigraphy through a wavelet-based decomposition of well log data. J Nat Gas Sci Eng, 40: 38–50

Kang Y S, Huangfu Y H, Zhang B, He Z P, Jiang S Y, Ma Y Z (2023). Gas oversaturation in deep coals and its implications for coal bed methane development: a case study in Linxing Block, Ordos Basin, China. Front Earth Sci (Lausanne), 10: 1031493

Karacan C O, Olea R A, Goodman G (2012). Geostatistical modeling of the gas emission zone and its in-place gas content for Pittsburgh-seam mines using sequential Gaussian simulation. Int J Coal Geol, 90: 50–71

Leuangthong O, McLennan J A, Deutsch C V (2004). Minimum acceptance criteria for geostatistical realizations. Nat Resour Res, 13: 131–141

Li J, Tang S H, Zhang S H, Li L, Wei J G, Xi Z D, Sun K (2018a). Characterization of unconventional reservoirs and continuous accumulations of natural gas in the Carboniferous-Permian strata, mid-eastern Qinshui basin, China. J Nat Gas Sci Eng, 49: 298–316

Li L J, Liu D M, Cai Y D, Wang Y J, Jia Q F (2021). Coal structure and its implications for coalbed methane exploitation: a review. Energy Fuels, 35(1): 86–110

Li R, Li G F (2022). Coalbed methane industry development framework and its limiting factors in China. Geofluids, 2022: 8336315

Li S, Tang D Z, Pan Z J, Xu H, Tao S, Liu Y F, Ren P F (2018b). Geological conditions of deep coalbed methane in the eastern margin of the Ordos Basin, China: implications for coalbed methane development. J Nat Gas Sci Eng, 53: 394–402

Li S, Qin Y, Tang D Z, Shen J, Wang J J, Chen S D (2023a). A comprehensive review of deep coalbed methane and recent developments in China. Int J Coal Geol, 279: 104369

Li W, Chen T J, Song X, Gong T Q, Liu M Y (2020). Reconstruction of critical coalbed methane logs with principal component regression model: a case study. Energy Explor Exploit, 38(4): 1178–1193

Li W, Zhang J G, Xie J, Xia Y, He Y L (2023b). Application of the wavelet transform and INPEFA in sequence stratigraphy. ACS Omega, 8(3): 3441–3451

Liang J T, Wang H L, Blum M J, Ji X Y (2019). Demarcation and correlation of stratigraphic sequences using wavelet and Hilbert-Huang transforms: a case study from Niger Delta Basin. J Petrol Sci Eng, 182: 106329

Liu B, Chang S L, Zhang S, Chen Q, Zhang J Z, Li Y R, Liu J (2022a). Coalbed methane gas content and its geological controls: research based on seismic-geological integrated method. J Nat Gas Sci Eng, 101: 104510

Liu D M, Jia Q F, Cai Y D, Gao C J, Qiu F, Zhao Z, Chen S Y (2022b). A new insight into coalbed methane occurrence and accumulation in the Qinshui Basin, China. Gondwana Res, 111: 280–297

Liu Y Y, Zhang X W, Guo W, Kang L X, Gao J L, Yu R Z, Sun Y P, Pan M (2022c). Research status of and trends in 3D geological property modeling methods: a review. Appl Sci, 12(11): 5688

Liu Z D, Zhao J Z (2016). Quantitatively evaluating the CBM reservoir using logging data. J Geophys Eng, 13(1): 59–69

Liu Z L, Chen D, Gao Z Y, Wu Y P, Zhang Y Z, Fan K Y, Chang B H, Zhou P, Huang W G, Hu C L (2023). 3D geological modeling of deep fractured low porosity sandstone gas reservoir in the Kuqa Depression, Tarim Basin. Front Earth Sci (Lausanne), 11: 1171050

Lu Y Y, Zhang H D, Zhou Z, Ge Z L, Chen C J, Hou Y D, Ye M L (2021). Current status and effective suggestions for efficient exploitation of coalbed methane in China: a review. Energy Fuels, 35(11): 9102–9123

Lv J T, Zhang M, Huai Y C, Tan C Q, Chen X T, Wang D A (2020). CBM reservoir log and fine geo-model analysis techniques: taking CBM in Surat basin as an example. J China Coal Soc, 45(5): 1824–1834 (in Chinese)

Ma P H, Shao X J, Huo M Y, Chu Q Z, Huo C L, Liang W B (2018). Concepts and methods for coalbed geology modeling: a case study in the Hancheng mining area, southeastern margin of Ordos Basin. Oil Gas Geol, 39(3): 601–610

Men X Y, Lou Y, Wang Y B, Wang Y Z, Wang L X (2022). Development achievements of China's CBM industry since the 13th Five–Year Plan and suggestions. Nat Gas Indust, 42(6): 173–178

Moore T A (2012). Coalbed methane: a review. Int J Coal Geol, 101: 36–81

Qin Y, Moore T A, Shen J, Yang Z B, Shen Y L, Wang G (2018). Resources and geology of coalbed methane in China: a review. Int Geol Rev, 60(5−6): 777–812

Quartero E M, Bechtel D, Leier A L, Bentley L R (2014). Gamma-ray normalization of shallow well-log data with applications to the Paleocene Paskapoo Formation, Alberta. Can J Earth Sci, 51(5): 452–465

Ren B, Zhang M, Cui Z H, Li C L, Xia Z H, Gan T, Lau H C (2016). A novel work flow of density-log normalization for coalbed-methane wells: an example from the Surat Basin in Australia. SPE Reservoir Eval Eng, 19(2): 205–213

Ren S P, Yao G Q, Zhang Y (2019). High-resolution geostatistical modeling of an intensively drilled heavy oil reservoir, the BQ 10 block, Biyang Sag, Nanxiang Basin, China. Mar Pet Geol, 104: 404–422

Rotimi O J, Ako B D, Wang Z L (2014). Reservoir characterization and modeling of lateral heterogeneity using multivariate analysis. Energy Explor Exploit, 32(3): 527–552

Salmachi A, Rajabi M, Wainman C, Mackie S, McCabe P, Camac B, Clarkson C (2021). History, geology, *in situ* stress pattern, gas content and permeability of coal seam gas basins in Australia: a review. Energies, 14(9): 2651

Shi X L, Cui Y J, Xu W K, Zhang J S, Guan Y Q (2020). Formation permeability evaluation and productivity prediction based on mobility from pressure measurement while drilling. Pet Explor Dev, 47(1): 146–153

Shu Y, Sang S X, Zhou X Z (2023). Geological modeling of coalbed methane reservoirs in the tectonically deformed coal seam group in the Dahebian block, western Guizhou, China. Front Earth Sci, 2023

Su Y F, Zhang Q H, Qu X R (2018). Evaluation on development potential of deep coalbed methane in middle-east area of Qinshui Coalfield. Coal Sci Technol, 46(5): 185–191

Tao S, Chen S D, Pan Z J (2019). Current status, challenges, and policy suggestions for coalbed methane industry development in China: a review. Energy Sci Eng, 7(4): 1059–1074

Teng J, Yao Y B, Liu D M, Cai Y D (2015). Evaluation of coal texture distributions in the southern Qinshui basin, north China: investigation by a multiple geophysical logging method. Int J Coal Geol, 140: 9–22

Wang G, Qin Y, Xie Y W, Shen J, Zhao L, Huang B, Zhao W Q (2018). Coalbed methane system potential evaluation and favourable area prediction of Gujiao blocks, Xishan coalfield, based on multi-level fuzzy mathematical analysis. J Petrol Sci Eng, 160: 136–151

Wang S, Shao L Y, Wang D D, Sun Q P, Sun B, Lu J (2019). Sequence stratigraphy and coal accumulation of Lower Cretaceous coal-bearing series in Erlian Basin, northeastern China. AAPG Bull,

103(7): 1653–1690

Wei Y L, Zhao L Y, Liu W, Zhang X, Guo Z J, Wu Z L, Yuan S H (2023). Coalbed methane reservoir parameter prediction and sweet-spot comprehensive evaluation based on 3D seismic exploration: a case study in western Guizhou Province, China. Energies, 16(1): 367

Xie W D, Gan H J, Chen C Y, Vandeginste V, Chen S, Wang M, Wang J Y, Yu Z H (2022). A model for superimposed coalbed methane, shale gas and tight sandstone reservoirs, Taiyuan Formation, Yushe-Wuxiang Block, eastern Qinshui Basin. Sci Rep, 12(1): 11455

Xu X K, Meng Z P, Wang Y (2019). Experimental comparisons of multiscale pore structures between primary and disturbed coals and their effects on adsorption and seepage of coalbed methane. J Petrol Sci Eng, 174: 704–715

Yao Y B, Liu D M, Tang D Z, Tang S H, Che Y, Huang W H (2009). Preliminary evaluation of the coalbed methane production potential and its geological controls in the Weibei Coalfield, southeastern Ordos Basin, China. Int J Coal Geol, 78(1): 1–15

Yong H, He W X, Guo B C (2020). Combining sedimentary forward modeling with sequential Gauss simulation for fine prediction of tight sandstone reservoir. Mar Pet Geol, 112: 104044–104115

Zeng B, Li M J, Shi Y, Wang X, Guo H, Ren J H, He X (2023). Delineation and quantification of effective source rocks using 3D geological modeling in a lacustrine basin. Geoenergy Sci Eng, 228: 211955

Zhang M, Fu X H, Zhang Q H, Cheng W P (2019). Research on the organic geochemical and mineral composition properties and its influence on pore structure of coal-measure shales in Yushe-Wuxiang Block, south central Qinshui Basin, China. J Petrol Sci Eng, 173: 1065–1079

Zhou F D, Allinson G, Wang J Z, Sun Q, Xiong D H, Cinar Y (2012). Stochastic modelling of coalbed methane resources: a case study in southeast Qinshui Basin, China. Int J Coal Geol, 99: 16–26

Zhou F D, Yao G Q, Tyson S (2015). Impact of geological modeling processes on spatial coalbed methane resource estimation. Int J Coal Geol, 146: 14–27

Zhou Y, Zhang S H, Tang S H, Yu T C, Feng Z (2020). Gas content modeling of No. 3 coal seam in district 3 of southern Shizhuang block. Coal Geol Explor, 48(1): 96–104 (in Chinese)

Zhu P, Ma T, Wang X, Li X, Dong Y, Yang W, Teng Z (2023). Wavelet transform coupled with Fischer plots for sequence stratigraphy: a case study in the Linxing area, Ordos Basin, China. Geoenergy Sci Eng, 231: 212306

AUTHOR BIOGRAPHIES

Xiongxiong YANG is a Ph.D candidate at China University of Geoscience, Beijing. He is mainly engaged in the exploration and development of unconventional natural gas, and currently focuses on the development of coalbed methane.
E-mail: yangxx@email.cugb.edu.cn

Shuheng TANG is a professor at China University of Geosciences, Beijing. His research interests include coal and coalbed methane geology, oil and gas field development geology, and unconventional oil and gas development theory and technology. He has published more than 200 peer-reviewed articles in professional journals and various academic conferences. As the first accomplisher or leading participant, he undertook more than 40 scientific research projects.
Email: tangsh@cugb.edu.cn

Songhang ZHANG is a professor at China University of Geosciences, Beijing. His research interest is coalbed methane geology and development. He is a member of the sixth Youth Working Committee of China Coal Society. He has published more than 60 peer-reviewed articles.
Email: zhangsh@cugb.edu.cn

Zhaodong XI is a research lecturer at China University of Geosciences, Beijing. He is mainly engaged in the exploration and development of unconventional natural gas, and currently focuses on the development of shale.
Email: xizhaod@cugb.edu.cn

Kaifeng WANG is a Ph.D candidate at China University of Geoscience, Beijing. He is mainly engaged in the exploration and development of unconventional natural gas, and currently focuses on the development of coalbed methane.
E-mail: wangkf@email.cugb.edu.cn

Zhizhen WANG is a Ph.D candidate at China University of Geoscience, Beijing. He is mainly engaged in the exploration and development of unconventional natural gas, and currently focuses on the development of coalbed methane.
E-mail: 2006200033@cugb.edu.cn

Jianwei LV is a Ph.D candidate at China University of Geoscience, Beijing. He is mainly engaged in the exploration and development of unconventional natural gas, and currently focuses on the development of coalbed methane.
E-mail: 276689740@qq.com